7

Differential-Absorption Lidar for Ozone and Industrial Emissions

Gary G. Gimmestad

Electro-Optics, Environment, and Materials Laboratory, 925 Dalney Street, Georgia Institute of Technology, Atlanta, Georgia 30332-0834, U.S.A. (gary.gimmestad@gtri.gatech.edu)

7.1 Introduction

During the first two decades of lidar development, much was accomplished with differential-absorption lidar, or DIAL. The basic theory was worked out, the relationship between signal-to-noise ratio and detection limits was elucidated, and DIAL systems in both the ultraviolet (UV) and infrared (IR) spectral regions were developed and fielded for ozone and industrial emissions including SO_2, NO_2, NH_3, HCl, CO, hydrazine, and Hg [1–3].

In the early days, building lidars was difficult and the technique developed a reputation as something of an arcane art. Even single-wavelength systems were complex and costly and they required highly trained operators and frequent adjustments. These problems were worse for DIAL and so, as promising as the early developments were, DIAL systems saw limited application. For broad acceptance, lidar systems in general needed simpler operation, better reliability, software to produce real-time reduced data, eye safety, standard measurement techniques, and lower costs. DIAL practitioners have made progress in all of these areas during the past two decades, and they have also developed better retrieval techniques and methods for greatly improving measurement accuracy.

In this chapter, the theory of the DIAL technique is reviewed first. Examples of the correction terms are given for the case of a UV ozone lidar, and the considerations for optimizing wavelengths are discussed. Progress in the development of DIAL techniques for ozone

and industrial emissions is then described in four wavelength regions: ultraviolet, visible, mid-infrared, and far infrared. Recent advances in multi-wavelength lidar are summarized, and finally, some conjectures are offered on technology areas that will most likely see rapid progress in the near future.

7.2 The DIAL Equation

We begin with the elastic backscatter lidar equation

$$P(R) = P_0 \eta \left(\frac{A}{R^2}\right)\left(\frac{c\tau}{2}\right)\beta(R)\exp\left[-2\int_0^R \alpha(r)\mathrm{d}r\right] \tag{7.1}$$

where $P(R)$ is the power received from range R, P_0 is the average transmitted power during the laser pulse, η is the receiver efficiency, A is the receiver area, R is the range to the scattering volume, c is the speed of light, τ is the laser pulse duration, and β and α are the atmospheric backscatter coefficient and atmospheric extinction coefficient at range R.

Next we consider a lidar operating at two wavelengths λ_{on} and λ_{off} where a trace gas of interest has correspondingly larger and smaller absorption cross sections, and we define P_{on} as the lidar signal at the wavelength λ_{on} and P_{off} as the signal at λ_{off}. For the purpose of illustration, we assume for the moment that the difference in the atmospheric extinction coefficients at the two wavelengths is solely due to the trace gas, that is,

$$\Delta\alpha = N\Delta\sigma \tag{7.2}$$

where N is the molecule number density of the trace gas and

$$\Delta\sigma = \sigma(\lambda_{\mathrm{on}}) - \sigma(\lambda_{\mathrm{off}}) \tag{7.3}$$

where σ is the molecular absorption cross section. We also assume that the atmospheric backscatter coefficients at the two wavelengths are identical. In this idealized case, after some algebraic manipulations, we find that

$$N = \frac{1}{2\Delta\sigma}\left[\frac{\mathrm{d}}{\mathrm{d}R}\ln\left(\frac{P_{\mathrm{on}}}{P_{\mathrm{off}}}\right)\right]. \tag{7.4}$$

Equation (7.4) shows that DIAL is a self-calibrating measurement technique: all instrument constants are removed by the sequential operations of forming a ratio, finding the logarithm, and taking the derivative

with respect to range. However, a word of caution is in order: the foregoing analysis assumes that there are no range-dependent differences in the lidar responses at the two wavelengths. Fredriksson and Hertz [4] provided an extensive summary of experimental problems that could cause systematic differences at the two wavelengths and consequent errors in the measured value of N, and Ismail and Browell [5] presented a thorough analysis of the sensitivity of DIAL measurements to both random signal errors and to differential cross section errors. The latter type of error arises from both atmospheric and system effects, including temperature and pressure sensitivities of the trace gas spectrum, Doppler broadening of the Rayleigh return, the non-zero width and a possible shift of the laser line, and uncertainties in its spectral purity and center wavelength. Although the analysis was for a water-vapor DIAL system operating at 720 nm, it can be applied to other gasses and wavelengths.

In practice, lidar signals are not recorded or analyzed as continuous functions, but rather as values in discrete range bins. Expressing the derivative in Eq. (7.4) in terms of a range increment ΔR, we have

$$N = \frac{1}{2\Delta\sigma\,\Delta R} \ln\left(\frac{P_{\text{off}}(R+\Delta R)}{P_{\text{off}}(R)} \frac{P_{\text{on}}(R)}{P_{\text{on}}(R+\Delta R)}\right). \qquad (7.5)$$

A real lidar system will have some limit with which it can resolve the term in parentheses in Eq. (7.5), and this fact sets the lidar's *limit of detection* N_{LD} for the gas of interest. Assuming that the smallest measurable value of the term in parentheses was 0.02 and using a range increment ΔR of 100 m, Collis and Russell [1] derived a table of DIAL detection limits for a combination of 14 gasses and wavelength pairs. Equivalently, Eq. (7.5) can be used in the design of a lidar to find the *minimum range resolution* ΔR_{min}, for a given value of $\Delta\sigma$.

Tropospheric DIAL data are usually recorded in fairly small range bins, typically 15 m, and analyzed with a range resolution of 50–300 m. The analysis is not done by simple differencing as in Eq. (7.5) but rather by various curve fitting and filtering techniques that are employed to increase the signal-to-noise ratio. The effect of these techniques on the range resolution actually obtained was studied by Beyerle and McDermid [6].

In the general case, the atmospheric backscatter coefficient is not the same at the two DIAL wavelengths and there is differential extinction due to air molecules, aerosols, and interfering gasses, in addition to the gas of interest. These wavelength-dependent effects require a set of

corrections to Eq. (7.5), as follows:

$$N = \frac{1}{2\Delta\sigma\,\Delta R}\left[\ln\left(\frac{P_{\text{off}}(R+\Delta R)}{P_{\text{off}}(R)}\frac{P_{\text{on}}(R)}{P_{\text{on}}(R+\Delta R)}\right)\right.$$
$$\left. - \ln\left(\frac{\beta_{\text{off}}(R+\Delta R)}{\beta_{\text{off}}(R)}\frac{\beta_{\text{on}}(R)}{\beta_{\text{on}}(R+\Delta R)}\right)\right] - D - E - F \qquad (7.6)$$

where

$$D = \frac{\Delta\alpha_{\text{mol}}}{\Delta\sigma} \qquad (7.7)$$

is due to the wavelength-dependent extinction of air molecules,

$$E = \frac{\Delta\alpha_{\text{aer}}}{\Delta\sigma} \qquad (7.8)$$

is due to the wavelength-dependent extinction of aerosols, and

$$F = \frac{N_{\text{IG}}\Delta\sigma_{\text{IG}}}{\Delta\sigma} \qquad (7.9)$$

is due to the wavelength-dependent extinction of an interfering gas. The quantity $\Delta\sigma_{\text{IG}}/\Delta\sigma$ is sometimes called the *cross sensitivity* Q_{IG}.

The molecular number density N, in units of molecules per m^3, is usually converted to a concentration C, or mass density, by multiplying with the mass M of one molecule:

$$C = MN. \qquad (7.10)$$

M in kg can be found from the molecular weight in atomic mass units (AMU) by using the relation $1\ \text{AMU} = 1.6605 \times 10^{-27}$ kg. A convenient and commonly used unit for concentrations of gaseous pollutants is $\mu\text{g/m}^3$. Sometimes mixing ratios are more practical quantities than concentrations because they remain unchanged when the temperature and pressure change. However, mixing ratios can be by weight or by volume, and this can cause confusion. The former are usually given in kg/kg, g/kg, etc. For the latter, units such as m^3/m^3 are not common; instead, percent (%, 10^{-2}), per mill (‰, 10^{-3}), parts per million (ppm, 10^{-6}), parts per billion (ppb, 10^{-9}), and parts per trillion (ppt, 10^{-12}) are used. Although mixing ratios are dimensionless numbers, it must be stated whether the ratios are by weight (as in ppmw) or by volume (as in ppmv), because the numbers are obviously not the same. The volume and mass mixing ratios of a gas with molecular number density

N and concentration C are simply given by N/N_{air}, and C/C_{air} with the molecular number density and the density of (dry) air at standard temperature and pressure (STP, 0 °C and 1.01325×10^5 Pa) being 2.687×10^{25} molecules/m^3 and 1.2929 kg/m^3, respectively.

A DIAL system is sensitive to N or C, not to the mixing ratio. In order to find a profile in terms of the mixing ratio (such as ppbv), the lidar investigator must have a profile of atmospheric density. Such profiles are often approximated from ground-level pressure and temperature measurements and standard atmospheric lapse rates. This process introduces additional uncertainty into the mixing ratio profile.

The correction terms D, E, and F in Eqs. (7)–(9) must be subtracted from the first term of Eq. (6). They are independent of the concentration of the gas of interest, and they are generally positive and not negligible. The magnitudes of the corrections can be illustrated with a specific example. We consider a typical UV DIAL system for tropospheric ozone (O_3), with λ_{on} equal to 288.9 nm and λ_{off} equal to 299.1 nm. These wavelengths are commonly used for ozone DIAL because they can be conveniently obtained from the fourth harmonic of a Nd:YAG laser (266 nm) by using stimulated Raman scattering (SRS) in high-pressure gas cells containing D_2 and H_2, respectively. These wavelengths are shown in Fig. 7.1, along with the UV spectrum of ozone. The spectrum of sulfur dioxide (SO_2) is also shown because it is an interfering gas. For this example, we consider the top of the mixing layer, taken to be at 2000 m above

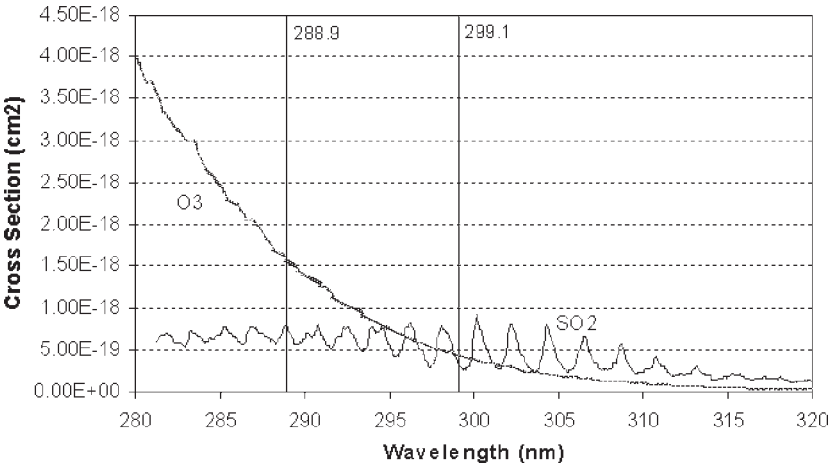

Fig. 7.1. Ultraviolet absorption spectra of ozone and sulfur dioxide.

ground level, where a steep gradient in the aerosol concentration often occurs. The concentration is assumed to decrease by a factor of $1/e^2$ in a vertical distance of 200 m. The aerosol properties in the mixed layer were calculated by assuming a visibility of 10 km at 550 nm, extinction-to-backscatter ratios S_{aer} ranging from 20 to 80 sr, and the Ångström exponent a ranging from 0 to 1. The variations in the correction terms (caused by variations of S_{aer} and a) are shown in Table 7.1. These correction terms are not small compared to typical urban daytime ozone values, which are on the order of 50–100 ppbv.

The backscatter gradient term is not simply additive as are terms D, E, and F. It is due to the difference in the total atmospheric backscatter coefficient at the two wavelengths. It is usually negligible in regions where backscattering is purely molecular in nature, but it becomes large at altitudes where large aerosol gradients exist. This is the primary reason that some DIAL systems employ a third wavelength to independently measure the aerosol profile. However, it should be noted that the early DIAL measurements preceded the development of aerosol inversion techniques that are now commonly used. Sasano, Browell, and Ismail [7] presented a full explanation for the inversion of lidar signals with both aerosol and Rayleigh backscatter in 1985. A useful algorithms for the correction of perturbations by aerosols has also been developed by Goers [8].

The role that aerosol profile inversion techniques play in the accuracy of DIAL results, particularly for the measurement of ozone, has been the topic of many discussions in the literature. Fujimoto, Uchino, and Nagai [9] and Godin et al. [10] systematically compared 4 and 10 different algorithms, respectively. Lidar ozone profiles were also compared with results of *in situ* measurements, showing that carefully taken lidar data differ no more from the results of *in situ* measurement devices than those results vary with respect to one another [11].

The molecular extinction term D is due to a difference in Rayleigh extinction and, consequently, it can be calculated accurately from the DIAL wavelengths and the air density. For this reason it does not present

Table 7.1. DIAL corrections for model atmosphere

Effect	Symbol	Correction
Backscatter gradient	—	29–39 ppbv
Molecular extinction	D	7 ppbv
Aerosol extinction	E	0 to >12 ppbv
Interfering gas	F	$0.4N_{SO_2}$

a major problem for lidar users and researchers. The sign of D is always positive when $\lambda_{on} < \lambda_{off}$.

The aerosol extinction term E is more problematic. As shown by the example summarized in Table 7.1, E takes values from 0 to 12 ppbv and beyond, depending on the aerosol optical properties, which are generally poorly known. This fact makes the value of E a large source of uncertainty.

The interfering gas term F can also be large. For the example shown, the cross sensitivity Q_{IG} between SO_2 and ozone is about 0.4. SO_2 arises largely from the combustion of fuels, and its concentration depends strongly on the types of fuels in use. In urban areas where high-sulfur coal is used, SO_2 concentrations on the order of 50 ppbv are not uncommon. This concentration would lead to a +20 ppbv error in the measured ozone concentration, for the values of λ_{on} and λ_{off} used in the example.

Proffitt and Langford [12] considered the optimization of λ_{on} and λ_{off} in detail for UV DIAL ozone lidar measurements in the free troposphere. The correction terms are small in the free troposphere, where large aerosol gradients are unusual and SO_2 concentrations are typically on the order of a few ppbv. Unfortunately, the corrections are largest in the mixed layer, where DIAL is a unique tool for measuring pollutants. Minimizing the uncertainties due to the correction terms is therefore especially important in the mixed layer.

As shown in Fig. 7.1, the sulfur dioxide cross section is highly structured in the wavelength region between 277 and 300 nm where most ozone DIAL measurements are made. Weitkamp and others [13] measured the SO_2 cross section in this range with <3 pm resolution and <4 pm accuracy. They defined 13 pairs of wavelengths, with differences $\Delta\lambda$ between 0.9 and 8.7 nm, for which the *differential* SO_2 cross section is zero within ±3% of each of the respective cross sections. If any of these wavelength pairs is used for ozone DIAL measurements, then the presence of SO_2 does not cause spurious higher-than-actual O_3 concentrations. Their wavelength pairs are listed in Table 7.2 in order of decreasing differential ozone cross section. The ozone cross sections are taken from Griggs [14].

We note that the correction terms of Eq. (6) all contain the factor $1/\Delta\sigma$, and that they all get larger as $\Delta\lambda$ becomes larger. It has thus been suggested that the ratio $\Delta\sigma/\Delta\lambda$ is a figure of merit that should be maximized (although this is just one consideration in choosing the best wavelength pair). For UV ozone lidar, Senff [15], developed the graphical presentation of $\Delta\sigma/\Delta\lambda$ shown in Fig. 7.2, which shows the relative

Table 7.2. Wavelength combinations for ozone DIAL at which the sulfur dioxide differential absorption cross section vanishes

	Wavelength pairs			Ozone absorption cross sections	
Pair	Signal wavelength λ_{on}, nm	Reference wavelength λ_{off}, nm	Wavelength difference $\lambda_{off} - \lambda_{on}$, nm	O_3 cross section at signal wavelength $\sigma(\lambda_{on})$, 10^{-23} m^2	Differential O_3 cross section $\sigma(\lambda_{on}) - \sigma(\lambda_{off})$, 10^{-23} m^2
A	280.9	289.6	8.7	35.4	20.8
B	277.6	284.1	6.5	46.4	20.6
C	280.9	288.3	7.4	35.4	18.3
D	277.6	282.7	5.1	46.4	16.7
E	278.6	282.9	4.3	42.3	12.6
F	284.1	289.6	5.5	25.8	11.2
G	277.6	280.9	3.3	46.4	11.0
H	282.9	286.4	3.5	29.7	8.9
I	286.4	289.6	3.2	20.8	6.2
J	280.9	282.7	1.8	35.4	5.7
K	282.7	284.1	1.4	29.7	3.9
L	286.4	288.3	1.9	20.8	3.7
M	278.6	279.5	0.9	42.3	2.1

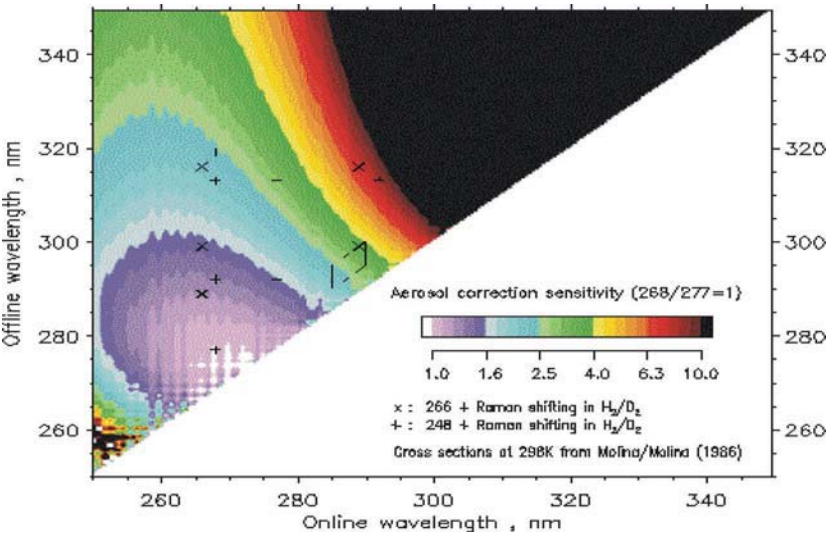

Fig. 7.2. Relative sensitivity to aerosol correction for various choices of λ_{on} and λ_{off} for UV ozone DIAL [15]. Ozone cross sections taken from Molina and Molina [16]. Crosses (+, ×) mark frequently used wavelength combinations.

values of this figure of merit for any choices of λ_{on} and λ_{off} between 250 and 350 nm. Note that *low* aerosol correction sensitivity represents a *large* figure of merit.

In Fig. 7.2 six popular wavelength combinations have been marked with crosses. Two of them are based on the krypton fluoride laser with the 268-nm deuterium first Stokes-shifted line as λ_{on} and the hydrogen first and second Stokes-shifted lines as $\lambda_{off}(+)$, four use the fourth harmonic of a Nd:YAG laser, both unshifted (266 nm) and first-Stokes-shifted in D_2 (289 nm), as λ_{on} and several Stokes-shifted lines from H_2 and D_2 as λ_{off}, $(\times)$. Ozone lidars have been reported that use for λ_{off} wavelengths as high as 316 nm, obtained from a second-Stokes Raman shift in D_2, but consideration of $\Delta\sigma/\Delta\lambda$ shows that such a choice of wavelengths is not a good practice. An appropriate value of $\Delta\sigma$ can be obtained, but the figure of merit is decreased substantially compared to shorter wavelengths, which means that the correction terms, and their uncertainties, are much larger.

Optimizing the choices of λ_{on} and λ_{off} for a given application requires a specification of the maximum range and the range resolution required, the spectra of the trace gas and any interfering gasses, and the expected concentrations of the trace gas and the interfering gasses. Wavelength optimization for UV ozone DIAL is achieved through the following considerations:

1. The ozone cross section at the wavelength λ_{on} must be low enough that the lidar can meet its maximum-range requirement.
2. The wavelengths λ_{on} and λ_{off} must be chosen so that $\Delta\sigma$ is large enough to meet the range resolution requirement [Eq. (5)].
3. The ratio $\Delta\sigma/\Delta\lambda$ should be maximized.
4. The wavelengths λ_{on} and λ_{off} should be chosen to minimize $\Delta\sigma_{IG}$.

As an example, an ozone DIAL system with a maximum range of 3 km and a range resolution of 200 m, for ozone concentrations up to 100 ppbv and SO_2 up to 50 ppbv, would have λ_{on} and λ_{off} in the 285 to 295 nm range with $\Delta\lambda$ about 5 nm. As mentioned above, $\Delta\sigma_{IG}$ can be made negligibly small by choosing a wavelength pair from Table 7.2.

In another case in which a shorter maximum range could be tolerated but higher O_3 concentrations had to be accommodated, the optimization led to the choice of $\lambda_{on} = 280.91$ nm and $\lambda_{off} = 282.72$ nm, i.e., wavelength pair *J* of Table 7.2. The individual steps of this optimization are described in detail in [8].

7.3 DIAL Systems

7.3.1 Ultraviolet DIAL Systems

The ultraviolet (UV) spectral region is useful for DIAL studies of pollution and industrial emissions because several pollutants have spectra in the UV region, because eye-safety requirements can be met in the UV, and because the sky background radiance is small, which makes daytime operation possible.

Ultraviolet DIAL systems have been developed and fielded in several countries around the world during the past two decades. Some of these lidars were in mobile vans, and the vans with the most published activity were developed in Sweden, first at the Chalmers Institute of Technology [17] and later at the Lund Institute of Technology [18]. All of the early Swedish mobile lidars were based on two Nd:YAG-pumped dye lasers, and all had a scanning mirror for mapping pollutant concentrations in horizontal or vertical slices.

In 1984, Swedish investigators reported a study of SO_2 from a paper mill that included concentration maps as well as an estimate of the flux of SO_2 from the mill [19], and in 1987 they mapped out NO_2 during an inversion episode that lead to a particularly high ground-level NO_2 concentration [20].

Edner and others [20] also reported measurements of molecular chlorine, Cl_2, using DIAL wavelengths in the 298–308 nm region. The UV spectrum of Cl_2 is featureless, so the problems involved in choosing DIAL wavelengths are somewhat like those for O_3 except that the cross section differences obtainable are about two orders of magnitude smaller for Cl_2. For this reason, the authors were only able to detect strong artificial sources of Cl_2. They also pointed out that their expected sensitivity using a 10-nm wavelength separation would be about seven times worse than that for NO_2 and that other gasses, such as O_3 and SO_2, would be strong interferents for open-atmosphere measurements. For these reasons, it is difficult to envision a practical application of UV DIAL for chlorine.

In 1989, the Swedish researchers reported DIAL monitoring of elemental mercury, Hg, pointing out that mercury is an unusual atmospheric pollutant because it occurs in elemental form [21]. Previous attempts had been made, but sensitive measurements had to await the availability of a high-power narrow-band laser at 254 nm, which was equipped with a dual-wavelength feature, producing on- and off-line pulses alternately. Mercury DIAL is complicated by the occurrence of

resonance fluorescence, so data processing must include some subtle differences from ordinary DIAL. The system was tested on plumes from a chlorine-alkali plant where mercury was used in the processing. Using the scanning DIAL system, the investigators mapped out the Hg plume and, with wind speed data, found the flux, which was 30 g/hr of atomic Hg. With a range resolution of 1 km, the investigators could measure concentrations on the order of 1 ng/m^3, which compares favorably with the average European background level of 1.6 ng/m^3.

Extensive improvements to the mobile van were reported in 2003 [22]. The lidar transmitter system is now all solid state, with two injection-seeded Nd:YAG lasers pumping optical parametric oscillators (OPOs) along with several harmonic generators to cover the wavelength range from 220 nm to about 4 μm. The van also incorporates instrumentation for laser-induced fluorescence (LIF) measurements on both aquatic and terrestrial targets.

Investigators in Germany developed a mobile UV DIAL van known as ARGOS (Advanced Remote Gaseous Oxides Sensor) [23]. ARGOS was designed to measure O_3, NO_2, and SO_2. The lidar is based on two Nd:YAG-pumped dye lasers, and the optical system includes a two-axis scanner. The ARGOS van also has a three-component Doppler sodar (sound detection and ranging) that measures the vertical profile of the wind vector for emission measurements and for investigations of transport phenomena in general. The ARGOS system is shown schematically in Fig. 7.3. The on and off wavelengths used are 296.17/297.35 nm for SO_2 and 280.92/282.72 nm for O_3. The rationale for these wavelength choices was described by Weitkamp and others [13].

Goers [24] described measurements of SO_2 and O_3 with ARGOS. The SO_2 measurements included emissions from a zinc smelter in Germany and steel mills in Brazil. As described earlier, DIAL measurements must be corrected for several error terms. An exceptionally detailed account of DIAL data processing, including aerosol correction algorithms, was given by Goers in her PhD thesis [8].

In the United States, a mobile DIAL van for use in air quality studies was constructed by the Environmental Technology Laboratory (ETL) of the National Oceanic and Atmospheric Administration (NOAA) [25–27]. The system, known as OPAL (Ozone Profiling Atmospheric Lidar), is quite different from the European vans because it was designed to obtain vertical distributions of one gas only, O_3. The lidar uses harmonics of Nd:YAG, Raman shifting with H_2 and D_2 (with both gasses in the same cell), and sum frequency mixing to generate 266, 289, 299, and

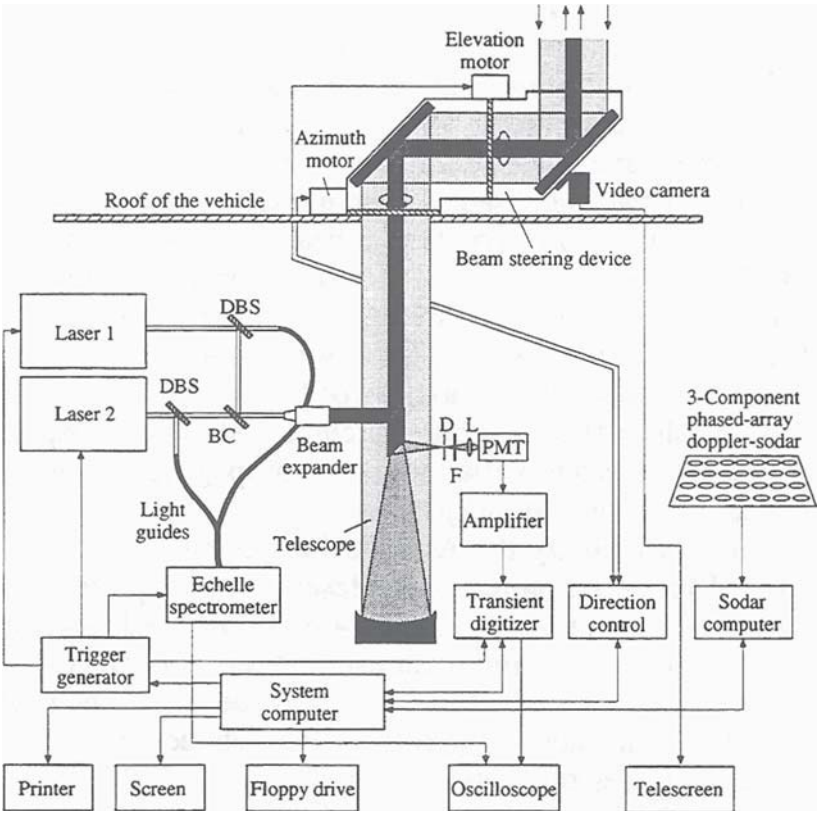

Fig. 7.3. The ARGOS system: DBS, dichroic beamsplitter; BC, polarizing beam combiner; D, diaphragm; F, filters; L, lens; PMT, photomultiplier tube [23].

355 nm. All wavelengths are transmitted simultaneously and separated in the receiver with filters and a spectrometer. The 355-nm signal is used to measure the aerosol profile. OPAL has been used in many air quality campaigns over the past decade, with continuous upgrades and improvements in its optical configuration.

A European system that, like OPAL, is exclusively for the measurement of ozone vertical profiles also employs Raman shifting, but it is based on a KrF excimer laser. The wavelength shifting occurs in one Raman cell only, and the first and second Stokes Raman lines of H_2 at 277.2 and 313.2 nm are used as the on- and off-resonance wavelengths [28].

Most European DIAL vans employ dye lasers for tunability whereas the NOAA OPAL system uses Raman shifting for compactness, simplicity and low maintenance effort. Ideally, a laser source would provide all of these attributes. The OPO is a compact, tunable, solid-state device that is starting to appear in lidar systems. In 2002, Fix and others [29] reported an extensive investigation of OPO sources for tunable UV radiation, using several different harmonics of Nd:YAG for both pumping the OPO cavity and for sum frequency mixing. These investigators obtained pulse energies up to 10 mJ in the 281–291 nm region and 4% conversion efficiency from the Nd:YAG fundamental at 1064 nm by utilizing intracavity mixing, as shown in Fig. 7.4. They enumerated the requirements of the OPO source for DIAL, including a robust design, easy handling, low cost, tunability, narrow linewidth, and wavelength stability. A lower-power version of their OPO source is used in the Ozone Profiler marketed by Elight Laser Systems of Teltow, Germany. The Ozone Profiler is an unattended system with an altitude range from 100 m up to 2 km.

Another O_3 DIAL system based on OPOs was reported by Zenker and others [30], who developed tunable OPO sources capable of transmitting as much as 25 mJ per pulse in the ultraviolet. The Swedish van also now uses OPOs, as mentioned above.

Lidar researchers at the Georgia Tech Research Institute in Atlanta, Georgia, are also developing an unattended O_3 DIAL system, in a partnership with LaserCraft, Inc. of Norcross, Georgia [31,32]. The Georgia

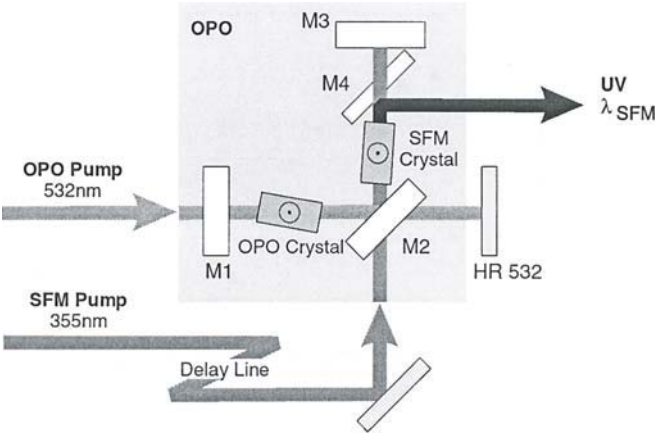

Fig. 7.4. Basic setup of the optical pametric oscillator (OPO) with intracavity sum-frequency mixing (SFM) [29].

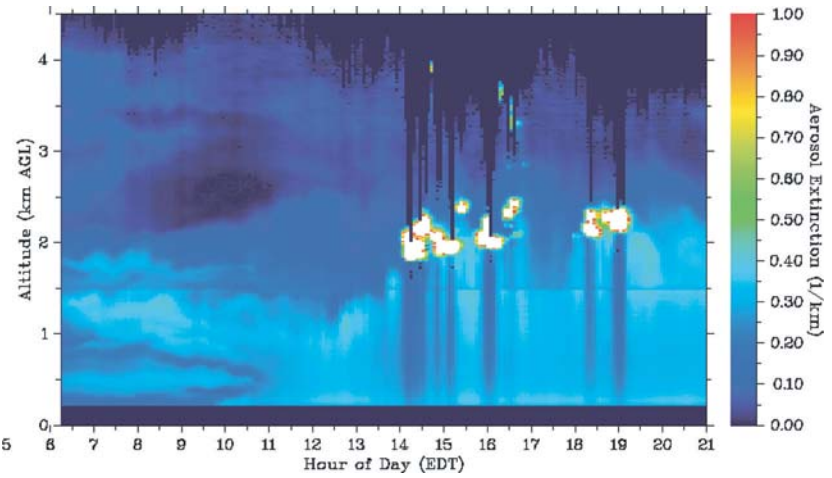

Fig. 7.5. Aerosol extinction profiles produced in real time by NEXLASER.

Tech system, known as NEXLASER (NEXt generation Laser Atmospheric sensor for the SouthEastern Region), is designed specifically for polluted urban environments. It has a maximum altitude of 3 km. NEXLASER is intended for deployment in networks of multiple units, providing real-time ozone profiles throughout an urban area to a central site via the Internet. The first version of the NEXLASER lidar was based on the NOAA OPAL system, using Raman shifting in H_2 and D_2 to obtain the DIAL wavelengths, which are susceptible to SO_2 as an interfering gas. Many urban environments have high concentrations of SO_2; for this reason, an OPO source is currently being investigated, along with other Raman-shifting gasses. NEXLASER features unattended operation and real-time reduced data, including both ozone profiles and aerosol extinction coefficient profiles. Examples are shown in Figs. 7.5 and 7.6.

7.3.2 Visible-Light DIAL Systems

The only application of visible-light DIAL to industrial emissions has been to nitrogen dioxide (NO_2), which has a spectrum with maximum cross section differences around 440 nm, as shown in Fig. 7.7. NO_2 is produced by combustion processes, and it is also the direct precursor of ozone.

Early estimates of the measurement precision of NO_2 lidars by Collis and Russell [1] and by Takeuchi and others [34] were not encouraging except for plumes, being in the range 100–1000 ppbv. However, the

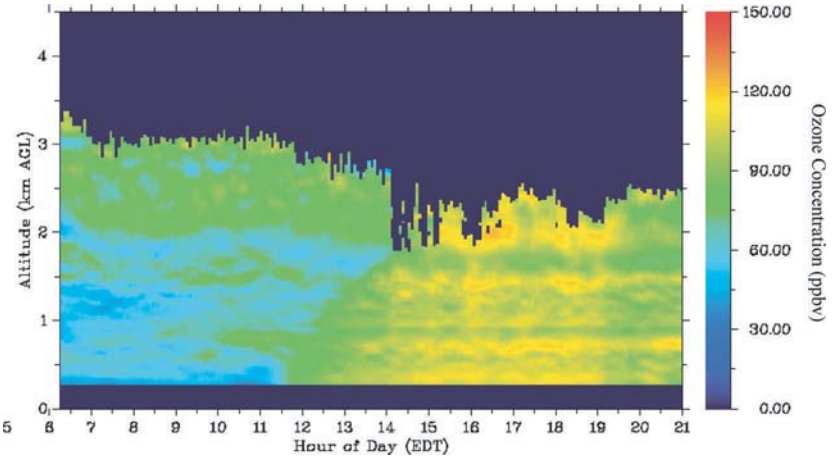

Fig. 7.6. Ozone profiles produced in real time by NEXLASER.

mobile DIAL system developed in Sweden [17] that used wavelengths near 448 nm was thoroughly evaluated by Fredriksson and Hertz [4], who found its measurement capabilities to be much better than the early estimates. Staehr and others [35] later demonstrated the detection of NO_2 to levels of 10 ppbv at ranges up to 6 km, with a two-laser system operating near 450 nm with near-simultaneous pulses at the two wavelengths. These authors also used what has come to be known as *null profiles* (recorded with both lasers tuned to the same wavelength) to determine their measurement uncertainties.

Kölsch and others [36] developed a concept in 1989 for simultaneously measuring NO and NO_2 with a pair of wavelengths near 454 nm

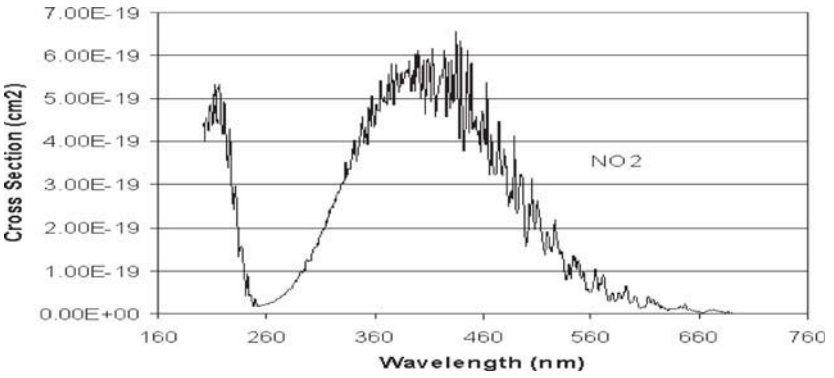

Fig. 7.7. The spectrum of NO_2 (from W. Schneider et al. [33]).

frequency-doubled to a pair near 227 nm. They demonstrated their idea with field measurements, using an excimer-pumped dye laser. In 1990 and 1991, Swart and other investigators reported a mobile NO_2 lidar in the Netherlands applied to emissions from stacks and freeway traffic [37, 38]. A mobile system was also built by Fritzsche and Schubert to simultaneously measure either two of the gases SO_2, NO_2, and O_3 or else one of those gases along with meteorological visual range [39].

Toriumi and others [40] reported an NO_2 lidar in 1996 that was based on a titanium:sapphire (Ti:Al_2O_3) laser operating at 447.9 nm (on) and 447.2 nm (off). The lidar, which was used to measure the exhaust plume from a diesel generator at a range of 125 m, had a range resolution of 12 m and a detection limit of 200 ppbv.

Yu and others [41] reported on a dual-wavelength Ti:sapphire laser and considered its use for NO_2 lidar, with on and off wavelengths of 398.3 and 397.5 nm, respectively. These wavelengths are just below the eye-safety cutoff at 400 nm, making eye-safe operation orders of magnitude easier to achieve. The transition to eye-safe operation may make NO_2 DIAL much more useful, especially in urban areas where it is difficult to ensure that personnel will never encounter the laser beam.

In Japan, Nayuki and others [42] recently developed an NO_2 lidar using sum frequency generation of 448-nm light with an Nd:YAG-pumped dye laser, and they reported measurements of concentrations in the range 10–50 ppbv at altitudes of 1–2 km, at night. They estimated their experimental error as ± 7 ppbv. The same authors later reported a DIAL system for simultaneous O_3 and NO_2 measurements with a measurement uncertainty of 5.5 ppbv in the 1.0–1.5 km altitude range [43]. These measurements were also made at night, because the sky background makes daytime measurements impractical.

Currently, eye-safe NO_2 lidars based on Ti:Al_2O_3 lasers are in use in Europe, and NO_2 lidars based on dye lasers are under development in Japan. Results to date show that measurement uncertainties on the order of 5 ppbv can be achieved at ranges of several km with range resolutions on the order of 100 m. Current eye-safe NO_2 DIAL systems are therefore useful for routine monitoring in polluted urban environments, where daytime NO_2 concentrations as high as 50 ppbv are not unusual.

7.3.3 Mid-Infrared DIAL Systems

Mid-IR DIAL measurements were made as early at 1980 by Weitkamp and others [44], who measured concentrations of hydrogen chloride

on the order of 1 ppm in the plume from a shipborne incinerator, by using a deuterium-fluoride (DF) laser to generate lines near 3.6 μm. In 1987, Menyuk and Killinger [45] reported a mid-IR lidar based on a Co:MgF_2 laser that was tunable from 1.5 to 2.3 μm, with a pulse energy of 10 mJ and 3 Hz pulse repetition frequency (PRF). The lidar receiver was based on a 0.3-m telescope with a cooled InSb detector. Extrapolating from measurements of HCl in a semi-enclosed cell at a concentration of 40 ppm, these investigators estimated that their lidar could measure HCl at concentrations of a few ppm at ranges of 2 km, and that the detection sensitivity for CH_4 would be an order of magnitude worse.

Milton and others [46] measured a range of organic and inorganic species including methane, propane and butane, along with other gasses amenable to lidar determinations in the UV and visible. They mixed radiation in the 785–851 nm region from a tunable dye laser with the output of a Nd:YAG laser to obtain IR radiation between 3.0 and 4.2 μm, which was then amplified in a pulsed optical parametric amplifier (OPA) [47].

Uchiumi and others [48] reported a mid-IR lidar based on a Raman-shifted Ti:Al_2O_3 laser, tunable from 680 nm to 3.2 μm. These authors found optimum wavelength pairs and calculated the maximum detection ranges for CH_4, CO_2, CO, and N_2O, finding that the maximum altitude ranges should be 2–3 km for all four gasses.

In 2000, Ambrico and others [49] published an extensive sensitivity analysis for mid-IR DIAL that included the following gasses: HCl, CO, CO_2, NO_2, CH_4, H_2O, and O_2 (as a reference gas). A wealth of DIAL line pairs was considered for three scenarios: clean air, urban polluted air, and stack emissions. The authors presented arguments that the mid-IR is a good wavelength region for DIAL measurements, particularly because tunable laser sources based on OPOs are now becoming available.

Despite the optimistic predictions of several investigators, few mid-IR DIAL measurements have been made to date. It is not yet clear whether routine DIAL measurements will eventually be made in the mid-IR.

7.3.4 Far-Infrared DIAL Systems

Quagliano and others [50] listed several advantages of the far-infrared region (8–12 μm) for gas detection, including the availability of CO_2 lasers that are line-tunable over much of this spectral region, the fact that many industrial gasses have unique far-IR spectra, and transparency of the atmosphere at these wavelengths. The authors investigated the

detection of trichloroethane, trichloroethylene, Freon 113, and ethylene, but their system measured only path-integrated concentrations because it relied on hard target returns. Ahlberg, Lundqvist, and Olsson [51] also described long-path measurements of ethylene using a CO_2 laser.

Force and others [52] reported laser remote sensing of ammonia (NH_3) with a CO_2 laser system, again using topographic targets. Their technique used the 10P(30) line at 10.69 μm and the 10P(32) line at 10.71 μm as the off and on lines, respectively. They were able to measure NH_3 concentrations from 5 to 20 ppbv with 30-s averaging. They also used the R(30) line at 9.22 μm and the R(26) line at 9.24 μm to measure NH_3 concentrations of 15 ± 5 ppbv by using a retroreflector at 2.7 km range.

In 1995, Carlisle and others [53] reported both hard-target and range-resolved measurements of chemical-vapor plumes using a CO_2-laser based DIAL system known as ADEDIS (from the French phrase *appareil de détection à distance*). They were concerned with the organophosphates triethylphosphate (TEP), diethylmethylphosphonate (DEMP), and di-isopropylmethylphosphonate (DIMP). They were able to measure TEP with a standard deviation of 0.13 mg/m^3 at a range of 1 km.

Barbini and others [54] described a dual-wavelength CO_2 laser for DIAL measurements and presented horizontal measurements of both O_3 and H_2O to a range of about 1 km. Their laser system transmitted about 300 mJ per pulse.

Although CO_2 lasers can provide numerous lines in the 9–11 μm region, the electronic noise associated with currently available detector/preamplifier combinations for direct detection is high and the atmospheric backscatter coefficient is generally very small. For these reasons, direct detection lidar in the far IR is insensitive and DIAL measurements are limited to ranges of about 1 km or less.

A 10-μm lidar can, of course, be made much more sensitive by using coherent detection. In 2002, Zhao and others [55] reported DIAL measurements with a coherent Doppler lidar in a field experiment with controlled releases of NH_3 plumes. The lidar was used to measure both wind speeds and NH_3 concentrations in the plumes, from which the investigators derived fluxes. Their measured fluxes were within 10% of the values calculated from the release rates, showing that their lidar technique can be used to find fluxes with a useful accuracy. Their measurement geometry and flux comparisons are shown in Figs. 7.8 and 7.9. Although the concentrations in the plume were rather large, Zhao [56] has shown that a different line pair could be used to measure

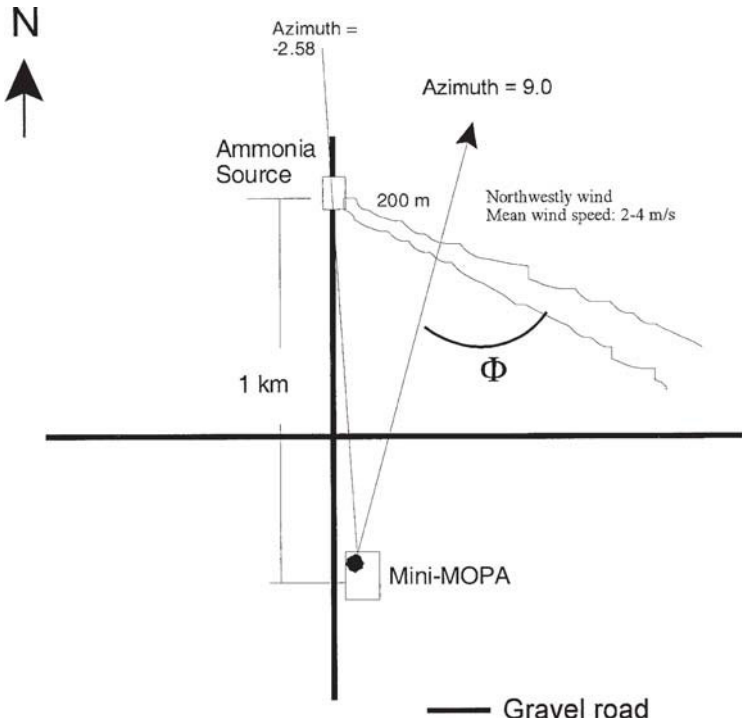

Fig. 7.8. Locations of the lidar and ammonia source and plume [55].

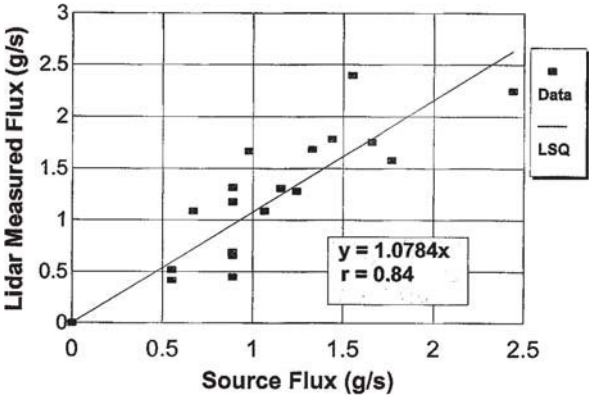

Fig. 7.9. Comparison of source fluxes with lidar-measured fluxes [55].

three-dimensional concentrations in the 5–100 ppbv range in an area 5 km on a side.

7.4 Multi-Wavelength DIAL

The DIAL technique can be viewed as a spectroscopic analysis reduced to its absolute minimum number of spectral elements, in which a gas concentration is determined from measurements at just two wavelengths, on and off the maximum of a spectral feature. By contrast, spectrometers commonly used in chemical analysis and in atmospheric studies employ thousands of spectral resolution elements to determine the concentrations of multiple gasses with overlapping spectra. Using more than two wavelengths is an obvious extension of the DIAL technique, yet multiple wavelengths have not been employed until recently, with the exception of line-tunable CO_2 laser systems using topographic targets. In addition to measuring more than one gas at a time, multiple wavelengths may also provide better knowledge of aerosol optical properties, which would improve the accuracy of aerosol corrections. New optimization schemes and new analysis algorithms will be needed for choosing the optimum wavelengths and to make full use of the additional data. The lidar community has just started to explore the advantages of multiple-wavelength systems.

Several different approaches to multiwavelength DIAL have been reported, including three-wavelength ozone lidar techniques to eliminate aerosol corrections and SO_2 interference, DIAL systems in which two gases are measured separately, three- and four-wavelength systems to provide immunity to an interfering gas or to otherwise improve measurement accuracy, and multiwavelength systems that measure two or more gasses simultaneously.

In 1985, Fredriksson [57] discussed the potential advantages of multiwavelength DIAL in connection with planned upgrades to the Swedish mobile lidar van, and the selection of a set of seven wavelengths in the mid-IR for the simultaneous measurement of methane, ethane, and propane was recently discussed by Weibring and others [22]. Warren [58] investigated the concept of using multiple wavelengths to measure multiple gasses by developing a methodology for estimating the detection and discrimination performance of a multiwavelength DIAL. Warren considered column content only, for two gasses. He found that a full matrix of uncertainty values was necessary because of correlations

in the statistical fluctuations of column content values, and pointed out that optimum wavelength values must be chosen with the matrix in mind.

Three-wavelength ozone measurements were proposed in 1994 and 1996 by Chinese investigators Wang and others [59, 60] who presented a theoretical analysis and a numerical simulation of a technique they termed *Dual DIAL*, proposing to use two pairs of lines that were obtainable from single-frequency lasers by Raman shifting. Their analysis showed that ozone measurements could be made much less sensitive to aerosol effects and also nearly immune to interference from SO_2 and NO_2 by using three wavelengths. Kovalev and Bristow [61] referred to Dual DIAL as a *compensational* technique, and discussed a three-wavelength version of it in which no correction is needed for aerosol differential extinction and backscattering. They also pointed out that errors due to interfering species could be decreased by a proper choice of wavelengths.

Rambaldi and others [62] reported five-wavelength DIAL measurements of SO_2 and O_3 using a system based on a Ce:LiSAF laser that was tunable from 284 to 299 nm. Their analysis was based on finding the SO_2 concentration first and then using it to correct the O_3 measurements, because they were measuring SO_2 concentrations as high as 1 ppmv whereas the O_3 concentration was only about 15 ppbv.

Strong and Jones [63] presented a theoretical analysis in 1995 for a novel instrument reported earlier by Jones [64]. The instrument employed a broadband, pulsed source (a xenon flash lamp), a spectrometer, and a CCD camera in order to generate range-resolved spectra. The authors used formal retrieval theory to estimate the errors in simultaneous profiles of O_3, H_2O, and NO_2, giving special attention to the effects of the flashlamp pulse duration and the CCD recording interval. They concluded that it should be possible to obtain vertical profiles of all three gasses simultaneously with 30% uncertainty up to altitudes of 12–15 km with a 3-km range resolution, using an integration time of 20 min. Apparently the technique is intended only for use in total darkness.

The most recent multiwavelength DIAL research has been conducted in Japan. Fukuchi and others [65, 66] investigated the use of multiple wavelengths to improve the accuracy of SO_2 measurements to the 1-ppbv level at 300 m resolution, which they adopted as requirements for studying transport. No reported SO_2 DIAL system had ever achieved this level of accuracy. They evaluated Dual DIAL using both three and four laser lines, and concluded that their desired accuracy should be achievable,

and that both aerosol effects and interference from ozone could be minimized by a proper choice of wavelengths.

Using a lidar system with two dual-wavelength tunable dye lasers, Fujii and others [67] actually achieved the predicted accuracy, measuring SO_2 at 2400–3000 m altitude to 1 ppbv with a range resolution of 300 m. Their system, which they called *MDIAL* for Multiwavelength DIAL, transmitted 10–18 mJ per pulse in the 298–300 nm region, and the receiver was based on a 500-mm-diameter telescope. They typically averaged the lidar returns from 1500 laser shots at each wavelength. The lidar was also capable of simultaneous measurements of multiple species by conventional two-wavelength DIAL, and they used this feature to experimentally evaluate the effect of O_3 on SO_2 measurements.

In 2002, the same group of Japanese researchers [68] presented a further improvement in which they developed curve-fitting techniques for use with multi-wavelength lidar measurements. They used five wavelengths around an SO_2 absorption peak, as shown in Fig. 7.10, to obtain both SO_2 and O_3 concentrations, and estimated that they could measure SO_2 concentrations with errors less than 0.5 ppbv at altitudes of about 1 km, with 300 m resolution. The researchers also compared the curve

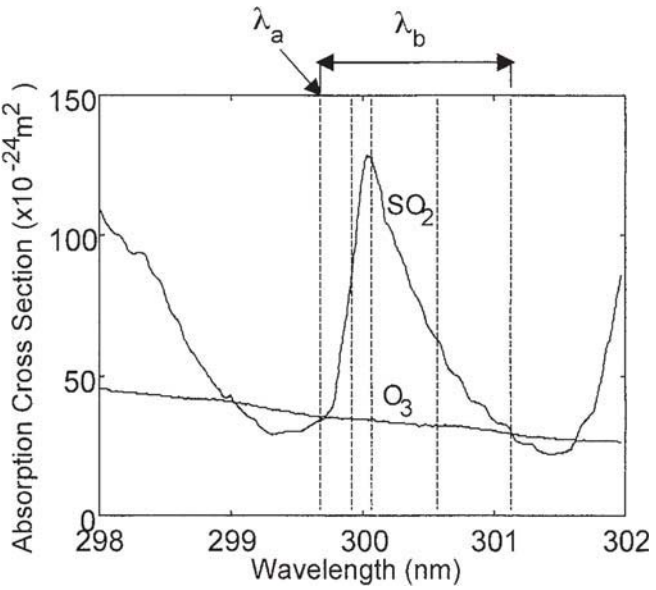

Fig. 7.10. Absorption cross sections for SO_2 and O_3 and the wavelengths used in the five-wavelength curve-fitting method for SO_2 [66].

fitting technique with Dual DIAL, and improved their choice of Dual DIAL wavelengths. The disadvantage of the curve fitting technique was a long measurement time (25 min for five wavelength pairs).

7.5 Outlook and Conclusions

Any lidar technique is dependent on the availability of suitable lasers, but for DIAL, the requirements are especially inflexible because the required laser characteristics are determined by the spectra of the molecules to be measured. The biggest problem has historically been to develop reliable lasers with outputs at appropriate wavelengths. Fortunately, steady progress is being made with tunable laser sources, especially OPOs. Tunable lasers enable researchers to optimize the wavelength choices and in that sense they are better than fixed-frequency wavelength shifters such as Raman cells. In addition, OPOs hold the promise of compact, all-solid-state systems that can, in principle, be developed for any wavelength from the UV to the far IR.

Continued progress can be expected in the area of multiwavelength DIAL; this area of research has already produced an order of magnitude improvement in DIAL sensitivity. Ultimately, one might expect that instruments and algorithms will be developed to obtain range profiles of multiple gasses simultaneously, along with aerosol characteristics.

Hybrid techniques, such as the Doppler DIAL measurements by NOAA described earlier, have begun to emerge and this trend may continue. For example, the micropulse lidar concept [69] could be combined with DIAL to develop an eye-safe lidar for NO_2 operating in the visible region around 448 nm. An effort to develop a DIAL micropulse lidar for water vapor has already been reported [70].

Remote monitoring of localized pollution sources such as plumes was demonstrated very early in the history of DIAL, and lidar techniques were later demonstrated for measuring pollutant fluxes and emission rates from wide-area sources such as industrial plants, particularly by researchers in Sweden and at NOAA. Further applications to large sources such as agricultural facilities and landfills are likely in the future.

DIAL systems for ozone and industrial pollution will no doubt continue to gain acceptance as costs become lower, reliability gets better, and algorithms to provide reduced data in real time are implemented in software. Another important issue discussed by Weitkamp and others [71] is the development of guidelines. The German Commission

on Air Pollution Prevention, KRdL, published guidelines for DIAL in 1999 [72]. The guidelines provide a foundation for lidar quality assurance and they are intended to help prospective users in several different ways. Guidelines and standards will undoubtedly play a key role in gaining acceptance for widespread applications of DIAL systems for air quality and emission monitoring.

References

[1] R.T.H. Collis, P.B. Russell: Lidar Measurement of Particles and Gases by Elastic Backscattering and Differential Absorption. In *Laser Monitoring of the Atmosphere*, E.D. Hinkley, ed. (Springer-Verlag, New York 1976), p. 102
[2] D.K. Killinger, A. Mooradian, eds.: *Optical and Laser Remote Sensing* (Springer-Verlag, New York 1983)
[3] R.M. Measures: *Laser Remote Sensing – Fundamentals and Applications* (Wiley, New York 1984)
[4] K.A. Fredriksson, H.M. Hertz: Appl. Opt. **23**, 1403 (1984)
[5] S. Ismail, E.V. Browell: Appl. Opt. **28**, 3603 (1989)
[6] G. Beyerle, I.S. McDermid: Appl. Opt. **38**, 924 (1999)
[7] Y. Sasano, E.V. Browell, S. Ismail: Appl. Opt. **24**, 3929 (1985)
[8] U.-B. Goers: Laserfernmessung von Schwefeldioxid und Ozon in der unteren Troposphäre mit Hilfe der differentiellen Absorption und Streuung unter den Bedingungen des mobilen Einsatzes und der besonderen Berücksichtigung des Einflusses von Grenzschichtaerosolen. PhD Thesis, Universität Hamburg (1994); Report GKSS 94/E/52 (1994)
[9] T. Fujimoto, O. Uchino, T. Nagai: In *17th International Laser Radar Conference. Abstracts of Papers. Sendai, Japan, July 25–29, 1994.* (Sendai International Center, Sendai, Japan 1994), p. 392
[10] S. Godin, A.I. Carswell, D.P. Donovan, et al.: Appl. Opt. **38**, 6225 (1999)
[11] C. Weitkamp, G. Baumbach, H. Becker, et al.: Gefahrstoffe-Reinhaltung der Luft **60**, 279 (2000)
[12] M.H. Proffitt, A.O. Langford: Appl. Opt. **36**, 2568 (1997)
[13] C. Weitkamp, O. Thomsen, P. Bisling: Laser und Optoelektonik **24** (2), 42 (1992)
[14] M. Griggs: J. Chem. Phys. **49**, 857 (1968)
[15] C. Senff: private communication 2001
[16] L.T. Molina, M.J. Molina: J. Geophys. Res. **91**, 14,501 (1986)
[17] K. Fredriksson, B. Galle, K. Nystrom, et al.: Appl. Opt. **20**, 4181 (1981)
[18] H. Edner, K. Fredriksson, A. Sunesson, et al.: Appl. Opt. **26**, 4330 (1987)
[19] A.-L. Egebeck, K.A. Fredriksson, H.M. Hertz: Appl. Opt. **23**, 722 (1984)
[20] H. Edner, K. Fredriksson, A. Sunesson, et al.: Appl. Opt. **26**, 3183 (1987)
[21] H. Edner, G.W. Faris, A. Sunesson, et al.: Appl. Opt. **28**, 921 (1989)
[22] P. Weibring, H. Edner, S. Svanberg: Appl. Opt. **42**, 3583 (2003)
[23] U.-B. Goers, P. Bisling, J. Glauer, et al.: ARGOS: A Differential Absorption Lidar for the Depth-Resolving Measurement of Sulfur Dioxide, Nitrogen Dioxide, and Ozone. In *Air Pollution Part II—Analysis, Monitoring, Management and*

Engineering, ed. by P. Zanetti, C.-A. Brebbia, J.E. Garcia Gardea, G. Ayala Milian (Computation Mechanics Publications, Boston 1993), p. 487
[24] U.-B. Goers: Opt. Eng. **34**, 3097 (1995)
[25] Y. Zhao, R.D. Marchbanks, R.M. Hardesty: Proc. SPIE **3127**, 53 (1997)
[26] Y. Zhao, R.M. Hardesty, M.J. Post: Appl. Opt. **45**, 7623 (1992)
[27] Y. Zhao, J.N. Howell, R.M. Hardesty: Proc SPIE **2112**, 310 (1993)
[28] W. Carnuth, U. Kempfer, T. Trickl: Tellus **54** B, 163 (2002)
[29] A. Fix, M. Wirth, A. Meister, et al.: Appl. Phys. B **75**, 153 (2002)
[30] J.T. Zenker, T.H. Chyba, C.L. McCray, et al.: Proc. SPIE **3707**, 541 (1999)
[31] J.M. Stewart, G.G. Gimmestad, D.W. Roberts, et al.: Proc. SPIE **4723**, 172 (2002)
[32] G.G. Gimmestad, E.M. Patterson, D.W. Roberts, et al.: *Proc. IEEE Int. Geosci. Remote Sensing Symp.* Sydney, Australia (2001)
[33] W. Schneider, et al.: J. Photochem. Photobiol. **40**, 195 (1987)
[34] N. Takeuchi, H. Shimizu, M. Okuda: Appl. Opt. **17**, 2734 (1978)
[35] W. Staehr, W. Lahmann, C. Weitkamp: Appl. Opt. **24**, 1950 (1985)
[36] H.J. Kölsch, P. Rairoux, J.P. Wolf, et al.: Appl. Opt. **28**, 2052 (1989)
[37] D.P.J. Swart, J.B. Bergwerff: In *Fifteenth International Laser Radar Conference. Abstracts of Papers. Tomsk, USSR, July 23–27, 1990.* (Institute Atmospheric Optics, Tomsk, USSR 1990), Part 1, p. 80.
[38] C.N. de Jonge, J.B. Bergwerff, D.P.J. Swart: Using DIAL to Measure Freeway Traffic NO_2 Emissions. In *Proceedings of the Optical Remote Sensing of the Atmosphere Topical Meeting*, Williamsburg, VA (1991), p. 250
[39] K. Fritzsche, G. Schubert: Laser und Optoelektronik **29** (5), 56 (1997)
[40] R. Toriumi, H. Tai, N. Takeuchi: Opt. Eng **35**, 2371 (1996)
[41] J. Yu, P. Rambaldi, J.-P. Wolf: Appl. Opt. **36**, 6864 (1997)
[42] T. Nayuki, T. Fukuchi, N. Cao, et al.: Appl. Opt. **41**, 3659 (2002)
[43] T. Fukuchi, T. Nayuki, N. Cao, et al.: Opt. Eng. **42**, 98 (2003)
[44] C. Weitkamp, H.J. Heinrich, W. Herrmann, et al.: Measurement of hydrogen chloride in the plume of incineration ships. In *Asociacion Argentina contra la Contaminacion del Aire, ed.: Proceedings of the 5th International Clean Air Congress*, 20–26 October 1980, Buenos Aires, Argentina (1980), p. 657
[45] N. Menyuk, D.K. Killinger: Appl. Opt. **26**, 3061 (1987)
[46] M.J.T. Milton, P.T. Woods, B.W. Joliffe, et al.: In *Sixteenth International Laser Radar Conference. Abstracts of papers presented at a conference and held in Cambridge, Massachusetts, July 20–24, 1992.* M.P. McCormick, ed. NASA Conference Publication 3158. Part 2, p. 711
[47] R.A. Robinson, P.T. Woods, M.J.T. Milton: Proc. SPIE **2506**, 140 (1995)
[48] M. Uchiumi, O. Chee, K. Muraoka, et al.: In *17th International Laser Radar Conference. Abstracts of Papers. Sendai, Japan, July 25–29, 1994.* (Sendai International Center, Sendai, Japan 1994), p. 31
[49] P.F. Ambrico, A. Amodeo, P.D. Girolamo, et al.: Appl. Opt. **39**, 6847 (2000)
[50] J.R. Quagliano, P.O. Stoutland, R.R. Petrin, et al.: Appl. Opt. **36**, 1915 (1997)
[51] H. Ahlberg, S. Lundqvist, B. Olsson: Appl. Opt. **24**, 3924 (1985)
[52] A.P. Force, D.K. Killinger, W.E. DeFeo, et al.: Appl. Opt. **24**, 2837 (1985)
[53] C.B. Carlisle, J.E. van der Laan, L.W. Carr, et al.: Appl. Opt. **34**, 6187 (1995)
[54] R. Barbini, F. Colao, G. D'Auria, et al.: Proc. SPIE **3104**, 167 (1997)
[55] Y. Zhao, W.A. Brewer, W.L. Eberhard, et al.: J. Atmos. Ocean Tech. **19**, 1928 (2002)

[56] Y. Zhao: Appl. Opt. **39**, 997 (2000)
[57] K.A. Fredriksson: Appl. Opt. **24**, 3297 (1985)
[58] R.E. Warren: Appl. Opt. **24**, 3541 (1985)
[59] Z. Wang, H. Hu, J. Zhou: In *17th International Laser Radar Conference. Abstracts of Papers. Sendai, Japan, July 25–29, 1994.* (Sendai International Center, Sendai, Japan 1994), p. 54
[60] Z. Wang, S. Zhou, H. Hu, et al.: Appl. Phys. B **62**, 143 (1996)
[61] V.A. Kovalev, M.P. Bristow: Appl. Opt. **35**, 4790 (1996)
[62] P. Rambaldi, M. Douard, J.-P. Wolf: Appl. Phys. B **61**, 117 (1995)
[63] K. Strong, R.L. Jones: Appl. Opt. **34**, 6223 (1995)
[64] R.L. Jones: Proc. SPIE **1715**, 393 (1992)
[65] T. Fukuchi, N. Goto, T. Fujii, et al.: Opt. Eng. **38**, 141 (1999)
[66] T. Fukuchi, T. Fujii, N. Goto, et al.: Opt. Eng. **40**, 392 (2001)
[67] T. Fujii, T. Fukuchi, N. Goto, et al.: Appl. Opt. **40**, 949 (2001)
[68] T. Fujii, T. Fukuchi, N. Cao, et al.: Appl. Opt. **41**, 524 (2002)
[69] J.D. Spinhirne: IEEE Trans. Geosci. and Remote Sensing **31**, 48 (1993)
[70] C. Oh, C.R. Prasad, V.A. Fromzel, et al.: Proc. SPIE **3707**, 177 (1999)
[71] C. Weitkamp, L. Woppowa, C. Werner, et al.: In *Lidar Remote Sensing in Atmosphere and Earth Sciences. Reviewed and revised papers presented at the twenty-first International Laser Radar Conference (ILRC21), Québec, Canada, 8–12 July 2002.* L.R. Bissonnette, G. Roy, G. Vallée, eds. (Defence R&D Canada Valcartier, Val-Bélair, QC, Canada), Part 1, p. 35
[72] Kommission Reinhaltung der Luft (KRdL) im VDI und DIN: Remote sensing / Atmospheric measurements with LIDAR / Measuring gaseous air pollutants with DAS LIDAR. **VDI 4210** Part 1, German/English (Beuth-Verlag, Berlin 1999)